Published in final edited form as:
Stem Cells. 2011 October ; 29(10): 1601–1610. doi:10.1002/stem.703.

Tumor Necrosis Factor Inhibits Mesenchymal Stem Cell Differentiation into Osteoblasts Via the Ubiquitin E3 Ligase Wwp1

Lan Zhao[a], **Jian Huang**[b], **Hengwei Zhang**[a], **Yi Wang**[a], **Lydia E. Matesic**[c], **Masahiko Takahata**[b], **Hani Awad**[b], **Di Chen**[b], and **Lianping Xing**[a]

[a]Department of Pathology and Laboratory Medicine, University of Rochester Medical Center, Rochester, New York, USA

[b]Department of Orthopaedics and Rehabilitation and Center for Musculoskeletal Research, University of Rochester Medical Center, Rochester, New York, USA

[c]Department of Biological Sciences, University of South Carolina, Columbia, South Carolina, USA

Abstract

Patients with chronic inflammatory disorders, such as rheumatoid arthritis, often have osteoporosis due to a combination of Tumor necrosis factor-induced increased bone resorption and reduced bone formation. To test if TNF inhibits bone formation by affecting the commitment and differentiation of mesenchymal stem cells (MSCs) into osteoblasts, we examined the osteogenic potential of MSCs from TNF transgenic (TNF-Tg) mice, a model of chronic inflammatory arthritis. MSC-enriched cells were isolated from bone marrow stromal cells using negative selection with anti-CD45 antibody coated magnetic beads. The expression profile of MSC surface markers the osteogenic, chondrogenic, and adipogenic properties of $CD45^-$ cells were confirmed by FACS and cell differentiation assays. MSC-enriched $CD45^-$ cells from TNF-Tg mice formed significantly decreased numbers of fibroblast and ALP^+ colonies and had a decreased expression of osteoblast marker genes. As TNF may upregulate ubiquitin ligases, which negatively regulate osteoblast differentiation, we examined the expression levels of several ubiquitin ligases and found that Wwp1 expression was significantly increased in MSC-enriched $CD45^-$ cells of TNF-Tg mice. Wwp1 knockdown rescued impaired osteoblast differentiation of TNF-Tg $CD45^-$ cells. Wwp1 promotes ubiquitination and degradation of JunB, an AP-1 transcription factor that positively regulates osteoblast differentiation. Injection of TNF into wild-type mice resulted in decreased osteoblast differentiation of MSCs and increased JunB ubiquitination, which was completely blocked in *Wwp1*$^{-/-}$ mice. Thus, Wwp1 targets JunB for ubiquitination and degradation in MSCs after chronic exposure to TNF, and inhibition of Wwp1 in MSCs could be a new mechanism to limit inflammation-mediated osteoporosis by promoting their differentiation into osteoblasts.

Correspondence: Lianping Xing, Ph.D., Department of Pathology and Laboratory Medicine, 601 Elmwood Ave, Box 626, Rochester, New York, NY 14642, USA. Telephone: 585-273-4090; Fax: 585-756-4468; lianping_xing@urmc.rochester.edu.

Disclosure of Potential Conflicts of Interest: The authors indicate no potential conflicts of interest.

Author contributions: L.Z. and J.H.: conception and design, collection and assembly of data, data analysis and interpretation, manuscript writing, final approval of manuscript; H.Z., Y.W., and M.T.: conception and design, data collection, data analysis, final approval of manuscript; L.E.M.: conception and design, provision of study material, manuscript writing, final approval of manuscript; H.A.: conception and design, provision of study material, final approval of manuscript; D.C.: conception and design, data analysis and interpretation, final approval of manuscript; L.X.: conception and design, financial support, data analysis and interpretation, manuscript writing, final approval of manuscript.

Keywords

Tumor necrosis factor; Mesenchymal stem cells; osteoblasts; Wwp1; E3 ligase

Introduction

Patients with chronic inflammatory disorders, such as Crohn's disease, systemic lupus erythematosus, and rheumatoid arthritis (RA), often have severe osteoporosis and increased incidence of bone fractures. Bone loss in these patients partly resulted from increased bone resorption, but is could also be contributed by impaired osteoblastic bone formation, the basis of which is less well understood. Patients with chronic inflammatory disorders often have increased levels of circulating tumor necrosis factor, a major inflammatory mediator. Many in vitro studies demonstrate that TNF is a strong osteoblast inhibitor via various mechanisms including the regulation of nuclear factor kappa-light-chain-enhancer of activated B cells, Runx2, and bone morphogenetic protein signaling molecules [1–4]. Recent in vivo studies suggest that Wnt signaling inhibitors such as dickkopf-1 and secreted frizzled-related proteins also play important roles in bone loss phenotypes of RA [5, 6]. Together, these in vitro and in vivo findings clearly indicate that (a) there is impaired osteoblast formation with TNF overexpression and (b) TNF-induced inhibition of osteoblast function operates through multiple mechanisms. However, these studies do not delineate at which stage of osteoblast differentiation TNF might start to act as a negative regulator.

Osteoblasts are derived from mesenchymal stem cells (MSCs) in the bone marrow, which are characterized by their ability to differentiate into various tissue lineages, including osteoblasts, adipocytes, and chondrocytes (among others). MSC research has been focused mainly on the generation and expansion of wild-type (WT and normal) MSCs for the purpose of tissue repair and regeneration. However, alteration of MSCs may play a critical role in various diseases, such as severe osteoporosis in RA, because impaired osteogenic potential of MSCs could reduce the number of osteoblast progenitors and ultimately lead to bone loss. Several studies have compared MSC function between RA patients and healthy subjects with various results [7]. These clinical reports often use bone marrow extracts, which contain many cell types, making the interpretation of results complicated. Here, we directly compared purified MSC-enriched population from TNF transgenic (TNF-Tg) mice, a model of RA, and WT littermates and demonstrated that TNF-Tg MSCs have reduced osteogenesis, which is accompanied by increased ubiquitin E3 ligase Wwp1-mediated JunB degradation.

Wwp1 belongs to the C2-WW-HECT subfamily of ubiquitin E3 ligases, which also includes Nedd4, Itch, Smurf1, Smurf2, and Wwp2. The best characterized function of ubiquitin E3 ligases is to recognize substrate proteins and to promote their ubiquitination and subsequent proteasomal degradation. We reported previously that Smurf1-mediated ubiquitination and degradation of BMP signaling proteins negatively regulates the function of mature osteoblasts in TNF-Tg mice [8–10]. However, it is not clear whether E3 ligases affect MSC function during chronic inflammation. In addition to its ubiquitin ligase activity, the WW domains of the protein have been shown to exhibit high affinity toward PY motifs and proline-rich sequences which mediate protein protein interactions between this class of E3s and their targets [11]. Although Wwp1 has been shown to be essential for embryonic development in *Caenorhabditis elegans* [12], *Wwp1*$^{-/-}$ mice are viable and fertile without any obvious abnormalities (our unpublished observations).

The role of Wwp1 in bone homeostasis was first suggested in the examination of the phenotype of *Schnurri-3* knockout mice (*Shn3*$^{-/-}$) by Jones et al. [13, 14]. *Shn3*$^{-/-}$ mice

develop severe osteosclerosis with dramatically increased bone mass. An in vitro assay indicates that Shn3 enhances Runx2 protein ubiquitination and degradation through the recruitment of Wwp1 to Runx2, leading to the hypothesis that Wwp1 mediates the osteosclerotic phenotype of *Shn3*$^{-/-}$ mice [13, 14]. However, whether or not Wwp1 plays a critical role in physiologic and pathologic bone loss in vivo is not known.

In this study, we demonstrated that MSC-enriched cells from TNF-Tg RA mice have reduced osteogenesis and increased Wwp1 expression. Wwp1 promotes the proteasomal degradation of JunB protein, a critical transcription factor which regulates the differentiation of MSCs into osteoblasts [15] upon TNF exposure. Thus, the inhibition of Wwp1 in MSCs could be a new mechanism to limit inflammation-mediated osteoporosis by promoting their differentiation into osteoblasts.

Materials and Methods

Animals

TNF-Tg (line 3647, on a C57BL/6 background) mice were obtained originally from Dr. G. Kollias (Vari, Greece). WT littermates and TNF-Tg mice used in this study were 6- to 10-month-old, an age when significantly reduced bone volume has been noted in these mice [8]. *Wwp1*$^{-/-}$ mice used for these studies were produced using standard knockout technology in embryonic stem cells. Characterization of these animals has revealed that they lack functional Wwp1 protein, is fully congenic on a C57BL/6 background, and is viable and fertile. Detailed description of *Wwp1*$^{-/-}$ mice will be published separately (Lydia E. Matesic et al., manuscript in preparation). All experiments described here were approved by the Institutional Animal Care and Use Committee at the University of Rochester Medical Center.

Plasmids and Antibodies

The Myc-Wwp1 plasmid was a gift from Dr. Ceshi Chen (Albany Medical College); the hemagglutinin (HA)-ubiquitin expression vector, the Flag-JunB expression vector, and the JunB-YF mutant vector have been described previously [9, 15, 16]. Monoclonal antibodies specific for Flag, HA, and β-actin were purchased from Sigma (St. Louis, MO, USA, www.sigmaaldrich.com); anti-JunB, anti-c-Myc, and anti-ubiquitin antibodies were from Santa Cruz (Santa Cruz, CA, USA, www.scbt.com); the anti-Wwp1 antibody was from Abnova Corporation (Walnut, CA, USA, www.abnova.com); the anti-Runx2 antibody was from MBL International (Woburn, MA, USA, www.mblintl.com); allophycocyanin (APC)-anti-CD45.2, fluorescein isothiocyanate (FITC)-anti-CD45.2, FITC-anti-CD11b, FITC-anti-CD31, R-Phycoerythrin (PE)-anti-CD29, PE-anti-CD105, PE-anti-CD106, APC-anti-CD44, and PE-Cy5-Sca-1 were purchased from eBioscience (San Diego, CA, USA, www.ebioscience.com).

Cell Cultures and MSC Isolation

Primary bone marrow stromal cells (BMSCs) were isolated according to our previously described methods [8, 9, 15]. Briefly, cells were cultured in α-minimal essential medium (MEM) with 10%–20% fetal bovine serum (FBS). MSC-enriched CD45^{-} cells were isolated from BMSCs derived from at least five mice. Cells from the second or third passage were used for all experiments. Cells were incubated with anti-CD45 antibody conjugated microbeads (Miltenyi Biotec, Auburn, CA, USA, www.miltenyibiotec.com). The CD45 negative population (CD45^{-}) was isolated by negative selection according to the manufacturer's instructions. Flow cytometry confirmed that more than 98% of isolated cells were CD45 negative (Supporting Information Fig. 1).

Osteogenic, Adipogenic, and Chondrogenic Differentiation

For osteogenesis, either $CD45^-$ or $CD45^+$ cells were cultured in the osteoblast-inducing medium containing 10% FBS, 5 mM β-glycerophosphate, and 100 μg/ml ascorbic acid in the presence or absence of BMP2. The dose of BMP2 varied with individual experimental conditions and is indicated in the figure legends. Alkaline phosphatase (ALP) staining was performed after culturing cells for 21 days. Bone nodule formation was examined in Alizarin red stained plates after 21–28 days in culture under these conditions. For adipogenesis, cells were cultured with the adipocyte differentiation medium for 12–16 days as described previously [17]. Adipocyte staining with oil red O was performed. For chondrogenesis, cell pellets were cultured with the chondrocyte differentiation medium (Hyclone, Rockford, IL, USA, www.thermoscientific.com) for 28 days. Cell pellets were fixed with 10% formaldehyde and embedded in paraffin. The sections were stained with Alcian Blue/hematoxylin/orange G.

CFU Assays

Bone marrow cells were isolated from the femurs of at least three mice per group and pooled. The colony-forming ability of bone marrow cells derived from WT and TNF-Tg mice or from WT and *Wwp1*$^{-/-}$ mice injected intraperitoneally with PBS or TNF (0.5 μg per injection, twice a day for 5 days) was compared. TNF injection did not affect cell viability (as show in Supporting Information Fig. 2). Bone marrow cells were combined, filtered, and then seeded in four 15-cm dishes at 1×10^7 cells per dish in media composed of α-MEM plus 15% FBS with β-glycerophosphate. After 25–28 days, cells were fixed in 10% formalin and subjected to ALP and eosin staining. The numbers of ALP^+ and total colonies (defined as containing at least 20 cells) were counted. For each experiment, results were normalized to the colony number counts obtained from either the WT or phosphate buffered saline (PBS)-injected WT samples as 100%. Data are presented as mean ± SD for the four dishes.

Ubiquitination Assays

Ubiquitination assays were performed as described previously [8, 15]. Briefly, 293T cells were transfected with HA-ubiquitin, Myc-WWP1, and either Flag-JunB or Flag-JunB-YF, and treated with MG132 (10 μM) for 4 hours before being harvested. Cell lysates were incubated with an anti-Flag antibody and protein G-agarose Sigma (St. Louis, MO, USA, www.sigmaaldrich.com) overnight at 4°C. The immunoprecipitates were subjected to Western blot analysis with an anti-HA antibody. BMSCs from mice that received TNF or PBS injection were treated with MG 132 (10 μM) for 4 hours and cell lysates were incubated with anti-JunB antibody and protein G agarose overnight at 4°C. The immunoprecipitates were subjected to Western blot analysis with an anti-ubiquitin antibody to detect the endogenous ubiquitination of JunB.

BrdU Incorporation

TNF-Tg and WT mice were in vivo labeled by administering two intraperitoneal injections of BrdU (1 mg/mouse/injection) spaced 16 hours apart, and euthanized 2 hours after the second injection. At that time, the bone marrow was harvested and treated with NH_4Cl to lyse red blood cells. The remaining cells were stained with APC-conjugated anti-CD44 and FITC-conjugated anti-BrdU for flow cytometry analysis using the FITC BrdU Flow Kit (BD Phamingen, San Diego, CA, www.bdbiosciences.com) according to the manufacturer's instructions. The percentage of $BrdU^+$ cells in the $CD45^-$ population was assessed.

Small Interfering RNAs (siRNA)

Wwpl siRNA and control siRNA were purchased from Santa Cruz. Three wells of MSC-enriched $CD45^-$ cells derived from TNF-Tg mice were transfected with *Wwpl* siRNA or control siRNA using DharmaFECT one (Thermo Scientific, Lafayette, CO, USA, www.dharmacon.com). Two days after transfection, cells were cultured in osteoblast differentiation medium with BMP-2 (200 ng/ml) for 4 days and then harvested for quantitative real time polymerase chain reaction (RT-PCR). Experiments were repeated three times with similar results.

Quantitative RT-PCR

Total RNA was prepared using the RNeasy Mini Kit (Qiagen, Germantown, MD, USA, www.qiagen.com) according to the protocol provided by the manufacturer. cDNAs were synthesized using the iSCRIPT cDNA Synthesis Kit (Bio-Rad, Hercules, CA, USA, www.bio-rad.com). Quantitative RT-PCR amplifications were performed in an iCycler (Bio-Rad, Hercules, CA, USA, www.bio-rad.com) RT-PCR machine using iQ SYBR Green supermix (Bio-Rad, Hercules, CA, USA, www.bio-rad.com). *β*-actin was amplified on the same plates and used to normalize the data. Each sample was prepared in triplicate and each experiment was repeated at least three times. The relative abundance of each gene was calculated by subtracting the C_T value of each sample for an individual gene from the corresponding C_T value of *β-actin* (ΔC_T). $\Delta\ \Delta C_T$ were obtained by subtracting the ΔC_T of the reference point. These values were then raised to the power of two ($2^{\Delta\Delta CT}$) to yield fold-expression relative to the reference point. Representative data are presented as means ± SD of the triplicates or of four wells of cell culture. The sequences of primer sets for *ALP*, *osteocalcin* (*OC*), *Smurf1*, *Smurf2*, *Shn3*, *Itch*, *Wwp1*, *JunB*, and *Runx2* mRNAs are shown in Table 1.

Statistical Analysis

Data are presented as mean ± SD, and all experiments were performed at least three times with similar results. Statistical analyses were performed with Stat view statistical software (SAS, Cary, NC, USA, www.sas.com). Differences between the two groups were compared using unpaired Student's *t* test, while more than two groups were compared using one-way analysis of variance between groups (ANOVA), followed by a Bonferroni/Dunnett's test. *p* values less than .05 were considered to be statistically significant.

Results

TNF-Tg Mice Have Decreased Mesenchymal Colony Formation

To determine if bone formation is inhibited in our TNF-Tg model of RA with severe osteoporosis, we compared serum osteocalcin levels and bone formation status of WT and TNF-Tg mice. TNF-Tg mice develop arthritis at 2- to 3-month-old and osteoporosis at about 4-month-old. The severity of arthritis and osteoporosis progresses with aging [8]. We found that TNF-Tg mice have significantly reduced serum osteocalcin levels, bone formation rate, and mineral apposition rate (Fig. 1B, 1C). These in vivo findings confirm that osteoblast function is indeed inhibited in TNF-Tg RA mice, making investigation of the molecular mechanism involved in obls in this model clinically significant.

To investigate whether increased expression of TNF has an effect on BMSCs, we isolated BMSCs from TNF-Tg mice and performed a colony-forming unit (CFU) assay, which is commonly used to study the proliferation and differentiation of BMSCs. Markedly, BMSCs from TNF-Tg mice formed less stromal colonies (CFU-F) than the WT cells (Fig. 1D, 1E), indicating decreased MSC activity in TNF-Tg mice. When these colonies were stained for

ALP activity (an osteoblast marker), TNF-Tg groups had less ALP^+ staining (Fig. 1D, 1E), suggesting that TNF overexpression may impair the osteoblast differentiation of BMSCs.

To determine whether such effects on BMSCs are caused by locally produced TNF or by globally circulating TNF, we injected TNF or PBS into WT mice for 5 days and harvested BMSCs for the CFU assay. Similar to what was found for the TNF-Tg mice, TNF injection also decreased the number of CFU-F and CFU-ALP^+ colonies significantly when compared with PBS injection (Fig. 1F, 1G). This suggests that globally circulating TNF alone has significant negative effects on mesenchymal colony formation and the potential of BMSCs to differentiate into osteoblasts. Thus, in terms of osteoblast differentiation, BMSCs may be negatively regulated by the TNF-rich, inflammatory microenvironment in the bone marrow.

This hypothesis was further substantiated upon determination of the mRNA levels of osteoblast markers *ALP* and *OC* in BMSCs derived from WT and TNF-Tg mice that had been cultured in the osteoblast differentiation medium in vitro for 14 days. We found that the BMSCs of TNF-Tg mice had similar expression levels of osteoblast marker genes at day 0 before differentiation. However, when compared with WT, significantly reduced expression of *ALP* and *OC* was observed in cells derived from TNF-Tg mice 14 days after culture in the osteoblast differentiation medium (Fig. 1H). Thus, BMSCs of TNF-Tg mice may have a decreased potential for osteoblast differentiation.

Characterization of BMSC Derived MSCs from Adult Mice

As BMSCs are regarded as a mixture of various cell types, among which only MSCs can differentiate into osteoblasts, we attempted to determine if the TNF effects, we observed previously (Fig. 1), were mediated via a direct regulation of MSCs in the BMSC mixture. To identify which subpopulation of the BMSCs represents MSCs, we stained BMSCs that had been cultured in vitro and passaged twice with DAPI and the following antibodies: FITC-conjugated anti-CD45, PE-conjugated anti-CD105, and biotin-labeled hematopoietic lineage flow cocktail (anti-CD3, CD45R/B220, CD11b, Ly6G, and erythroid marker) using flow cytometry. Analysis of the resulting scatter plots revealed that 99.2% of $CD45^-$ cells were hematopoietic lineage negative. When the $CD45^-$ population was specifically gated, it was determined that 52.8% of this population was $CD105^+$, a marker specifically expressed in MSCs [18, 19] (Fig. 2A). Thus, $CD45^-$ BMSCs could be considered to be an MSC-enriched population.

This was further validated by characterizing $CD45^-$ BMSC isolated by affinity selection. Using micro-beads conjugated with an antibody that recognizes mouse CD45, $CD45^+$ BMSCs were separated from $CD45^-$ BMSCs. Successful selection of both $CD45^+$ and $CD45^-$ populations was confirmed with flow cytometry (Supporting Information Fig. 1). Given these results, this technique was subsequently used throughout this study to obtain MSC-enriched $CD45^-$ cells from BMSCs. Osteoblast, adipocyte, and chondrocyte differentiation of these MSC-enriched $CD45^-$ cells were carried out. Phenotypic assays such as ALP, Alizarin red, oil red O, and Alcian Blue staining demonstrated that only the $CD45^-$, but not the $CD45^+$ cells, retained the MSC ability to differentiate into osteoblasts, adipocytes, or chondrocytes (Fig. 2B). Furthermore. characterization of these $CD45^-$ MSC-enriched cells by flow cytometry confirmed that they were positive for MSC markers such as CD29, CD105, CD106, CD44, Sca-1, but did not express non-MSC markers like CD31 and CD11b (Fig. 2C). Thus, the $CD45^-$ population of BMSCs isolated using CD45 beads was enriched in MSCs and could therefore be used to study MSC function.

MSC-Enriched CD45⁻ Cells Derived from TNF-Tg Mice Have Decreased Osteogenic Potential

Next, we isolated MSC-enriched CD45⁻ cells from WT mice, and treated these cells with either PBS or TNF. ALP staining was decreased in the TNF-treated group when compared with the PBS-treated group (Fig. 3A), indicating that TNF could decrease the ability of MSCs to differentiate into osteoblasts. ALP staining of MSC-enriched CD45⁻ cells derived from TNF-Tg mice also showed decreased osteoblast differentiation compared with CD45⁻ cells obtained from WT BMSCs (Fig. 3B, left). We also measured the ALP activity of CD45⁻ cells and found that TNF-Tg-derived CD45⁻ cells had significantly lower ALP activity than WT cells (Fig. 3B, right). Furthermore, the mRNA expression of osteoblast makers *ALP* and *OC* was significantly lower in TNF-Tg CD45⁻ cells than in the WT cells (Fig. 3C). Interestingly, BrdU incorporation in CD45⁻ cells of TNF-Tg and WT bone marrow was comparable (Fig. 3D), suggesting that osteoblast differentiation of MSCs, but not proliferation, is impaired upon exposure to TNF.

Increased Ubiquitin E3 Ligase Wwp1 Expression in BMSCs and MSC-Enriched CD45⁻ Cells Derived from TNF-Tg Mice

It was reported that proteasome inhibitor treatment can promote MSC differentiation into osteoblasts [17], suggesting that the ubiquitin-proteasome pathway may play a negative role in osteoblast differentiation. Because MSCs exposed to TNF had impaired osteoblast differentiation, we proposed that this might be mediated through the upregulation of a C2-WW-HECT E3 ligase, which could promote degradation of factors important to osteogenesis. We found that the expression levels of *Shn3* and *Wwp1* mRNA were increased when either WT BMSCs (Fig. 4A) or the preosteoblast cell line 2T3 (Supporting Information Fig. 3) was cultured in the osteoblast differentiation medium while the expression of *Smurf1* and *Smurf2* were not changed, demonstrating a correlation of osteoblast differentiation with changes in *Shn3* and *Wwp1* expression. Thus, we performed quantitative RT-PCR to investigate if mRNA expression of C2-WW-HECT E3 ligase genes is increased in TNF-Tg cells when compared with WT cells. Using BMSCs, we demonstrated that *Wwp1* was significantly increased in TNF-Tg cells, while the expressions of other ubiquitin ligases remained unchanged compared with WT cells (Fig. 4B). We confirmed the upregulation of *Wwp1* expression in MSC-enriched CD45⁻ cells derived from TNF-Tg mice through analysis of both mRNA (Fig. 4C) and protein levels (Fig. 4C, insert). It should be noted that Shn3, which was reported to be an adaptor protein recruited by Wwp1 to induce Runx2 degradation, was not induced in TNF-Tg BMSCs and MSC-enriched CD45⁻ cells, suggesting that Shn3 may not be required for Wwp1 function in mesenchymal progenitor cells.

To test if Wwp1 is a key regulator in the TNF-mediated inhibition of osteogenesis, we knocked down *Wwp1* expression by transfecting CD45⁻ cells harvested from TNF-Tg mice with *Wwp1* siRNA. *Wwp1* mRNA expression was decreased by 95% when cells were transfected with *Wwp1* siRNA when compared with cells receiving control siRNA. Interestingly, *Wwp1* knockdown increased the expression of *ALP* and *OC* more than twofold in TNF-Tg cells, suggesting that the downregulation of *Wwp1* can rescue osteoblast differentiation of TNF-Tg MSC-enriched cells (Fig. 4D). Together, our results suggest that Wwp1 negatively regulates differentiation of MSCs into osteoblasts following exposure to TNF.

Wwp1 Induces JunB Ubiquitination and Degradation

To search for endogenous targets of Wwp1 in MSCs that may be responsible for impaired osteogenesis, we examined the protein levels of Runx2 and JunB, two critical factors controlling osteoblast differentiation that both possess a “PY” motif, through which a

substrate protein can be recognized by HECT-type ubiquitin ligases [15, 20]. As shown in Figure 5A (Supporting Information Fig. 4), TNF-Tg-derived MSC-enriched CD45$^-$ cells had a twofold increase in Wwp1 protein and a threefold decrease in JunB protein levels compared with WT-derived cells. In contrast, Runx2 protein levels were similar between WT and TNF-Tg CD45$^-$ cells. Quantitative RT-PCR was also performed to examine mRNA expression of *Wwp1*, *JunB*, and *Runx2*. While *Wwp1* expression was induced in TNF-Tg CD45$^-$ cells, *JunB* and *Runx2* expression was unchanged (Fig. 5B). Therefore, the decreased JunB protein level could be the direct consequence of post-translational regulation of JunB by Wwp1, which might be ubiquitin-proteasome related. To test this hypothesis, we transfected 293T cells with Wwp1 and JunB expression plasmids and found that Wwp1 overexpression decreased JunB protein levels by almost fourfold, suggesting that Wwp1 may be targeting JunB for degradation (Fig. 5C). To test if JunB is degraded through the ubiquitin-proteasome pathway, we carried out ubiquitination assays in the presence of proteasome inhibitor MG132 and found that Wwp1 could induce the ubiquitination of JunB (Fig. 5D). Thus, we conclude that Wwp1 mediates JunB ubiquitination and degradation upon TNF exposure to inhibit MSC differentiation into osteoblasts.

TNF-Induced Effects on Mesenchymal Colony Formation, Osteoblast Differentiation, and JunB Ubiquitination Are Abolished in Wwp1$^{-/-}$ Mice

To confirm that Wwp1 is responsible for mediating the effects of TNF exposure on mesenchymal colony formation and osteoblast differentiation of BMSCs in vivo, we injected TNF or PBS into *Wwp1*$^{-/-}$ mice and WT littermates, using the same protocol outlined in Figure 1G. BMSCs were isolated and CFU assays were performed. We found that BMSCs derived from both PBS- and TNF-treated *Wwp1*$^{-/-}$ mice formed more colonies than those derived from WT mice, suggesting that Wwp1 is a negative regulator of osteoblast differentiation (Fig. 6A). Significantly, Wwp1 deficiency rescued BMSCs from the inhibitory effects of TNF with regards to colony formation, suggesting that TNF downregulates osteoblast differentiation through Wwp1 (Fig. 6A). We then performed RT-PCR to examine the mRNA expression of osteoblast markers *ALP* and *OC* and found that mRNA expressions of both *ALP* and *OC* were increased in BMSCs (Fig. 6B) from *Wwp1*$^{-/-}$ mice relative to WT littermates. Consistent with the results of the CFU assays, the inhibitory effect of TNF on osteoblast marker gene expression was almost completely abrogated in cells derived from *Wwp1*$^{-/-}$ mice (Fig. 6B).

As Wwp1 is an ubiquitin ligase that is induced in MSCs by exposure to TNF and its target protein JunB positively reg-ulates osteoblast differentiation, we hypothesized that cells obtained from *Wwp1*$^{-/-}$ animals would have less ubiquitination of JunB proteins than comparable cells derived from WT littermates, and TNF treatment could increase JunB ubiquitination, which should be abolished when WWP1 is absent. Thus, we performed ubiquitination assays on BMSCs from PBS- or TNF-treated *Wwp1*$^{-/-}$ and WT mice. As expected, markedly increased JunB ubiquitination was observed in BMSCs from TNF-injected WT mice, but not in the cells har-vested from *Wwp1*$^{-/-}$ mice (Fig. 6C). Furthermore, the basal level of JunB ubiquitination was also abolished in *Wwp1*$^{-/-}$ cells (Fig. 6C), suggesting that Wwp1 is responsible for basal and TNF-induced JunB ubiquitination and degradation, and JunB is an endogenous target of Wwp1 in BMSCs. Taken together, these experiments suggest that TNF-mediated MSC inhibition is mediated by Wwp1 in vivo.

Discussion

In this study, we identified a population of MSC-enriched CD45$^-$ cells derived from the BMSCs of mice with TNF-induced chronic arthritis with significantly reduced osteogenic capacity. We found that expression levels of the ubiquitin E3 ligase Wwp1 were increased in

TNF-Tg MSC-enriched CD45$^-$ cells, and that knocking down *Wwp1* corrected the osteogenic differentiation defect in TNF-Tg cells. Furthermore, we showed that increased Wwp1 in TNF-Tg CD45$^-$ cells is accompanied by decreased protein levels of the AP1 protein JunB, a transcription factor critical for osteoblast formation. Wwp1 promotes the ubiquitination and proteasomal degradation of JunB protein. Wwp1 deficiency prevented TNF from impairing MSC differentiation into osteoblasts and inducing JunB ubiquitination. Taken together, these data indicate that chronic TNF exposure decreases the osteogenic potential of MSCs by increasing Wwp1-mediated JunB protein degradation, and this may be one of the molecular mechanisms underlying systemic bone loss seen in patients with chronic inflammation.

Accumulating evidence suggests that MSCs may decrease destructive inflammation, reduce tissue loss, and enhance the tissue repair process. In mice with collagen-induced arthritis, intravenous injection of WT MSCs reduces joint inflammation [21]. With greater uptake of MSC-based therapeutics in various diseases including autoimmune diseases, it will be important to determine whether the MSCs derived from patients with chronic inflammatory disorders, most of them being autoimmune in etiology, function normally. Here, we demonstrate that MSCs obtained from mice subjected to chronic TNF exposure have significantly reduced osteogenic potential. This finding is consistent with a recent study using MSCs from a mouse model of systemic lupus erythematosus. BMSCs from systemic lupus erythematosus mice have significantly reduced osteoblast differentiation [22]. However, our findings differ from published results using short-term TNF in vitro treatment of MSCs, in which TNF increases ALP activity [23], induces a chemotactic effect, and stimulates production of anti-inflammatory and growth factors, such as hepatocyte growth factor [24], insulin growth factor, and vascular endothelial growth factor [25]. Thus, endogenous chronic TNF exposure may have a different effect on MSC function than does in vitro TNF treatment.

Wwp1 is a member of the C2-WW-HECT family of E3 ligases. We have reported previously that Smurf1, another member of this family, negatively regulates the function of mature osteoblasts in TNF-Tg mice [8] and speculated that a chronic inflammatory environment increases the function or expression of a subset of E3 ligases, leading to the degradation of a group of positive regulators of osteogenesis. In *Shn3*$^{-/-}$ mice, Wwp1 is proposed to be an E3 ligase which mediates Runx2 degradation by binding to Shn3, explaining the osteosclerosis phenotypes observed in *Shn3*$^{-/-}$ mice [14]. However, this mechanism may not be operational in MSCs. MSCs express very low levels of Runx2, and we detected no difference in Runx2 protein levels between MSC-enriched CD4$^-$ cells derived from TNF-Tg mice when compared with WT littermates, suggesting that, at this stage, the expression of Runx2 protein is suppressed. Therefore, this protein modification mechanism likely does not apply to Runx2 at this stage. Alternatively, Runx2 is also known to be regulated by JunB [26], which is expressed at relatively high levels in MSCs. Further, JunB can be regulated via Smurf1-mediated ubiquitination and proteasomal degradation [15]. Unlike Runx2, we found that JunB protein levels are reduced in TNF-Tg CD45$^-$ cells and this is accompanied by an elevation in Wwp1 (Fig. 5A). However, Smurf1 levels are comparable in MSC-enriched CD45$^-$ cells derived from TNF-Tg or from WT mice (Fig. 4) although its expression is increased in mature osteoblasts of TNF-Tg mice [9]. Thus it is possible that increased levels of Wwp1 inhibit the osteogenic potential of MSCs while elevated Smurf1 reduces the function of mature osteoblasts. Together, these inhibitory mechanisms result in severe systemic bone loss in TNF-Tg mice and patients with RA.

Ubiquitin protein ligases have largely been considered to be constitutively active and regulated only at the level of target binding. However, it has recently become evident that HECT-type E3 ligases can be regulated by other mechanisms, including phosphorylation of

the ligase or substrate, utilization of adaptor proteins, or intramolecular and intermolecular interactions [27–29]. A few E3 ligases are regulated at the transcriptional levels. TNF and glucocorticoid dexmethasone upregulate the expression of MuRF1/MAFbx expression (two muscle-specific ubiquitin ligases) [30], possibly via the activation of NF-κB [31]. Induction of these ligases is essential for TNF-induced muscle loss in mice [32]. We reported that TNF increases the expression of Smurf1 in osteoblasts, but this takes 3 days, suggesting an indirect mechanism [9]. Currently, we do not know the mechanism of TNF-induced *Wwp1* expression, which needs to be studied further.

Several signaling pathways have been implicated in TNF-mediated inhibition of osteoblast function, including BMP/Smads, NF-κB, and Wnt/β-catenin. Although it has not been extensively studied as to whether these same pathways also affect MSC function in vivo under chronic TNF exposure condition, it is likely that Wwp1 is not the only mechanism for inhibiting the osteogenic potential of MSCs. Furthermore, ubiquitin E3 ligases usually have multiple target proteins and likely influence multiple pathways. In the future, it will be interesting to determine if post-translational modifications mediated by Wwp1 influences key signaling pathways in both MSCs and osteoblasts.

Conclusion

The MSC-enriched $CD45^-$ population isolated from mice with TNF-induced arthritis has significantly reduced osteogenic differentiation potential and increased expression levels of the ubiquitin E3 ligase Wwp1. Wwp1 negatively regulates MSC differentiation to osteoblasts by promoting proteasomal degradation of the JunB protein. Our findings raise two important points regarding MSCs obtained from patients with chronic inflammation disorders and autoimmune diseases: (a) MSCs from these patients are not normal in term of osteogenesis and (b) inhibition of Wwp1 may represent a new therapy for inflammatory osteoporosis.

Supplementary Material

Refer to Web version on PubMed Central for supplementary material.

Acknowledgments

We thank Dr. Ceshi Chen (Albany Medical College) for providing the Myc-Wwp1 plasmid and anti-WWP1 antibody. This work was supported by Grants R21-AR53586 and R01-AR48697 (to L.X.) from NIH.

References

1. Canalis E. Effects of tumor necrosis factor on bone formation in vitro. Endocrinology. 1987; 121:1596–1604. [PubMed: 3665833]
2. Li YP, Stashenko P. Proinflammatory cytokines tumor necrosis factor-alpha and IL-6, but not IL-1, down-regulate the osteocalcin gene promoter. J Immunol. 1992; 148:788–794. [PubMed: 1309841]
3. Nanes MS. Tumor necrosis factor-alpha: Molecular and cellular mechanisms in skeletal pathology. Gene. 2003; 321:1–15. [PubMed: 14636987]
4. Gilbert L, He X, Farmer P, et al. Expression of the osteoblast differentiation factor RUNX2 (Cbfa1/AML3/Pebp2alpha A) is inhibited by tumor necrosis factor-alpha. J Biol Chem. 2002; 277:2695–2701. [PubMed: 11723115]
5. Diarra D, Stolina M, Polzer K, et al. Dickkopf-1 is a master regulator of joint remodeling. Nat Med. 2007; 13:156–163. [PubMed: 17237793]
6. Walsh NC, Reinwald S, Manning CA, et al. Osteoblast function is compromised at sites of focal bone erosion in inflammatory arthritis. J Bone Miner Res. 2009; 24:1572–1585. [PubMed: 19338457]

7. Dudics V, Kunstar A, Kovacs J, et al. Chondrogenic potential of mesenchymal stem cells from patients with rheumatoid arthritis and osteoarthritis: Measurements in a microculture system. Cell Tissue Organ. 2009; 189:307–316.
8. Guo R, Yamashita M, Zhang Q, et al. Ubiquitin ligase Smurf1 mediates tumor necrosis factor-induced systemic bone loss by promoting proteasomal degradation of bone morphogenetic signaling proteins. J Biol Chem. 2008; 283:23084–23092. [PubMed: 18567580]
9. Kaneki H, Guo R, Chen D, et al. Tumor necrosis factor promotes Runx2 degradation through up-regulation of Smurf1 and Smurf2 in osteoblasts. J Biol Chem. 2006; 281:4326–4333. [PubMed: 16373342]
10. Xing L, Zhang M, Chen D. Smurf control in bone cells. J Cell Biochem. 2010; 110:554–563. [PubMed: 20512916]
11. Verdecia MA, Joazeiro CA, Wells NJ, et al. Conformational flexibility underlies ubiquitin ligation mediated by the WWP1 HECT domain E3 ligase. Mol Cell. 2003; 11:249–259. [PubMed: 12535537]
12. Huang K, Johnson KD, Petcherski AG, et al. A HECT domain ubiquitin ligase closely related to the mammalian protein WWP1 is essential for *Caenorhabditis elegans* embryogenesis. Gene. 2000; 252:137–145. [PubMed: 10903445]
13. Jones DC, Wein MN, Glimcher LH. Schnurri-3: A key regulator of postnatal skeletal remodeling. Adv Exp Med Biol. 2007; 602:1–13. [PubMed: 17966382]
14. Jones DC, Wein MN, Oukka M, et al. Regulation of adult bone mass by the zinc finger adapter protein Schnurri-3. Science. 2006; 312:1223–1227. [PubMed: 16728642]
15. Zhao L, Huang J, Guo R, et al. Smurf1 inhibits mesenchymal stem cell proliferation and differentiation into osteoblasts through JunB degradation. J Bone Mineral Res. 2010; 25:1246–1256.
16. Shen R, Chen M, Wang YJ, et al. Smad6 Interacts with Runx2 and mediates Smad ubiquitin regulatory factor 1-induced Runx2 degradation. J Biol Chem. 2006; 281:3569–3576. [PubMed: 16299379]
17. Huang J, Zhao L, Xing L, et al. MicroRNA-204 regulates Runx2 protein expression and mesenchymal progenitor cell differentiation. Stem Cells. 2010; 28:357–364. [PubMed: 20039258]
18. Mukherjee S, Raje N, Schoonmaker JA, et al. Pharmacologic targeting of a stem/progenitor population in vivo is associated with enhanced bone regeneration in mice. J Clin Invest. 2008; 118:491–504. [PubMed: 18219387]
19. Kolf CM, Cho E, Tuan RS. Mesenchymal stromal cells. Biology of adult mesenchymal stem cells: Regulation of niche, self-renewal and differentiation Arthritis Res Ther. 2007; 9:204.
20. Rotin D, Kumar S. Physiological functions of the HECT family of ubiquitin ligases. Nat Rev Mol Cell Biol. 2009; 10:398–409. [PubMed: 19436320]
21. Mao F, Xu WR, Qian H, et al. Immunosuppressive effects of mesenchymal stem cells in collagen-induced mouse arthritis. Inflamm Res. 2010; 59:219–225. [PubMed: 19763787]
22. Sun L, Akiyama K, Zhang H, et al. Mesenchymal stem cell transplantation reverses multiorgan dysfunction in systemic lupus erythematosus mice and humans. Stem Cells. 2009; 27:1421–1432. [PubMed: 19489103]
23. Ding J, Ghali O, Lencel P, et al. TNF-alpha and IL-1beta inhibit RUNX2 and collagen expression but increase alkaline phosphatase activity and mineralization in human mesenchymal stem cells. Life Sci. 2009; 84:499–504. [PubMed: 19302812]
24. Zhang A, Wang Y, Ye Z, et al. Mechanism of TNF-alpha-induced migration and hepatocyte growth factor production in human mesenchymal stem cells. J Cell Biochem. 2010; 111:469–475. [PubMed: 20533298]
25. Crisostomo PR, Wang Y, Markel TA, et al. Human mesenchymal stem cells stimulated by TNF-alpha, LPS, or hypoxia produce growth factors by an Nf Kappa B- but not JNK-dependent mechanism. Am J Physiol Cell Physiol. 2008; 294:C675–682. [PubMed: 18234850]
26. Lee KS, Hong SH, Bae SC. Both the Smad and p38 MAPK pathways play a crucial role in Runx2 expression following induction by transforming growth factor-beta and bone morphogenetic protein. Oncogene. 2002; 21:7156–7163. [PubMed: 12370805]

27. Wiesner S, Ogunjimi AA, Wang HR, et al. Autoinhibition of the HECT-type ubiquitin ligase Smurf2 through its C2 domain. Cell. 2007; 130:651–662. [PubMed: 17719543]

28. Gao M, Karin M. Regulating the regulators: Control of protein ubiquitination and ubiquitin-like modifications by extracellular stimuli. Mol Cell. 2005; 19:581–593. [PubMed: 16137616]

29. Gallagher E, Gao M, Liu YC, et al. Activation of the E3 ubiquitin ligase Itch through a phosphorylation-induced conformational change. Proc Natl Acad Sci USA. 2006; 103:1717–1722. [PubMed: 16446428]

30. Li YP, Chen Y, John J, et al. TNF-alpha acts via p38 MAPK to stimulate expression of the ubiquitin ligase atrogin1/MAFbx in skeletal muscle. FASEB J. 2005; 19:362–370. [PubMed: 15746179]

31. Cai D, Frantz JD, Tawa NE Jr, et al. IKKbeta/NF-kappaB activation causes severe muscle wasting in mice. Cell. 2004; 119:285–298. [PubMed: 15479644]

32. Adams V, Mangner N, Gasch A, et al. Induction of MuRF1 is essential for TNF-alpha-induced loss of muscle function in mice. J Mol Biol. 2008; 384:48–59. [PubMed: 18804115]

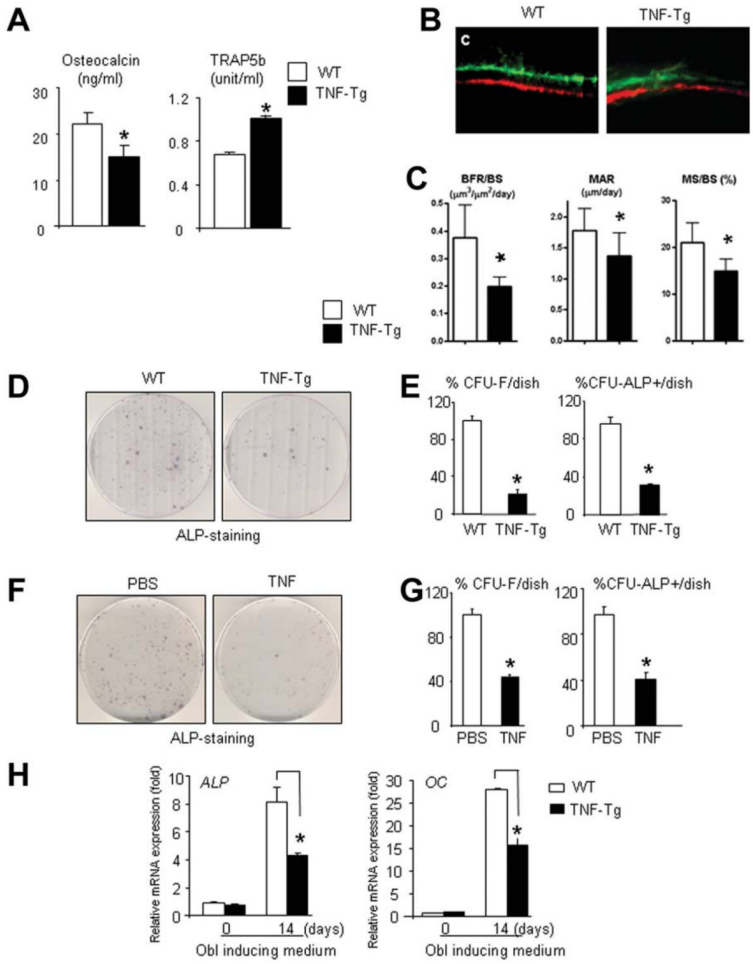

Figure 1.

TNF-Tg mice have decreased osteoblastic bone formation and mesenchymal colony formation. Serum bone formation and resorption markers were measured in 5- to 7-month-old TNF-Tg and wild-type (WT) mice by ELISA (enzyme-linked immunosorbent assay). Bars are the mean of SD of 18 mice per genotype **(A)**. Representative images of fluorochrome-markers double labeled trabecular bone at distal metaphysic of femur in WT and TNF-Tg mice **(B)**. Histomorphometric analysis. Bars are the mean of SD of eight mice per genotypes **(C)**. Bone marrow stromal cells (BMSCs) from TNF-Tg mice and WT littermates **(D, E)** or from WT mice injected with TNF or PBS **(F, G)** were cultured in the osteoblast differentiation medium for 25–28 days in a colony formation assay. Cells were fixed and stained with eosin or for alkaline phosphatase (ALP) activity **(D, F)**. Representative colony-forming unit (CFU)-ALP$^+$ colonies are shown in **(E, G)**. The numbers of CFU-F (eosin staining) and CFU-ALP$^+$ colonies were counted and normalized to the WT or PBS-injected WT samples. Bars represent the mean ± SD of four dishes per genotype. **(F):** BMSCs from WT and TNF-Tg mice were cultured in the osteoblast differentiation medium and *ALP* and *OC* mRNA levels were examined by real time-polymerase chain reaction. Values shown are the mean ± SD of triplicates. The fold increase was calculated by dividing the values from different groups by the value of WT cells at day 0 as 1. *, $p < .05$ versus cells of WT or PBS-injected mice. The experiments were repeated three times with similar results. Abbreviations: ALP, alkaline phosphatase; BFR, bone formation rate; BS, bone surface; CFU, colony-forming unit; MAR, mineral apposition rate;

MS, mineralizing surface; OC, osteocalcin; PBS, phosphate buffered saline; TNF, tumor necrosis factor; WT, wild-type.

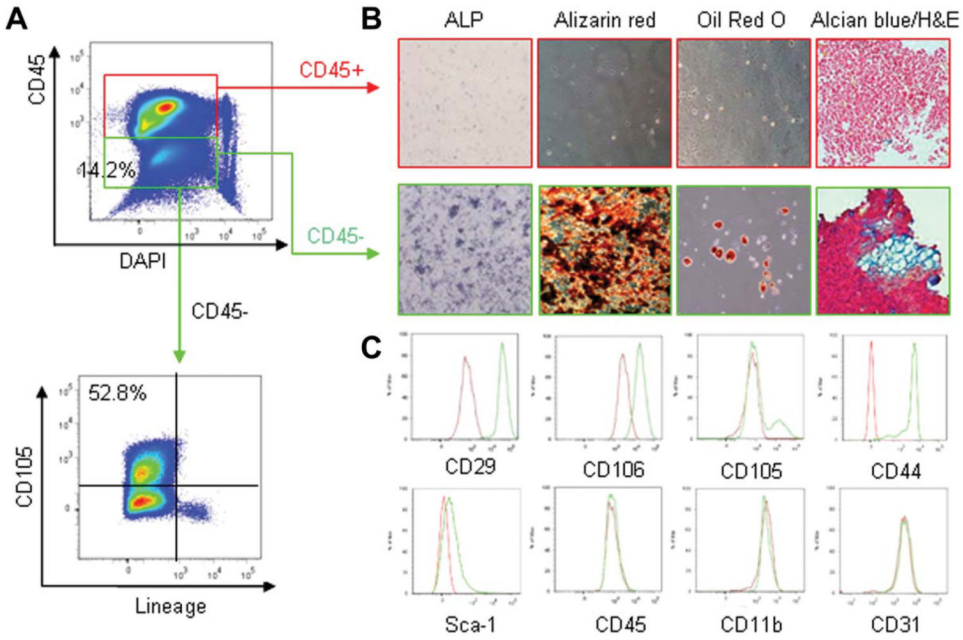

Figure 2.

Characterization of a mesenchymal stem cell (MSC)-enriched population derived from bone marrow stromal cells (BMSCs) of adult mice. Wild-type BMSCs were cultured in α-minimal essential medium, passaged twice, and subjected to flow cytometry after staining with FITC-anti-CD45, PE-anti CD105, biotin labeled hematopoietic lineage flow cocktail, and DAPI. **(A):** Scatter plots show that 99.2% of $CD45^-$cells are lineage negative and 52.8% of them are $CD105^+$. **(B):** $CD45^+$ hematopoietic lineage cells and $CD45^-$ MSC-enriched cells were purified using microbeads conjugated with an anti-CD45 antibody. Purified cells were cultured in osteoblast, adipocyte, or chondrocyte differentiation medium. Alkaline phosphatase (an osteoblast marker), Alizarin red (marker of matrix mineralization), oil red O (lipid), and Alcian Blue (chondrocyte) staining were performed. **(C):** $CD45^-$ cells were stained with PE-anti-CD105, allophycocyanin (APC)-anti-CD45, fluorescein isothiocyanate (FITC) -anti-CD11b, FITC-anti-CD31, PE-anti-CD29, APC-anti-CD44, PE-cy5-Sca-1, and FITC-anti-CD106 and then subjected to flow cytometry. The experiments were repeated once with similar results. Abbreviations: ALP, alkaline phosphatise; DAPI, 4′,6-diamidino-2-phenylindole.

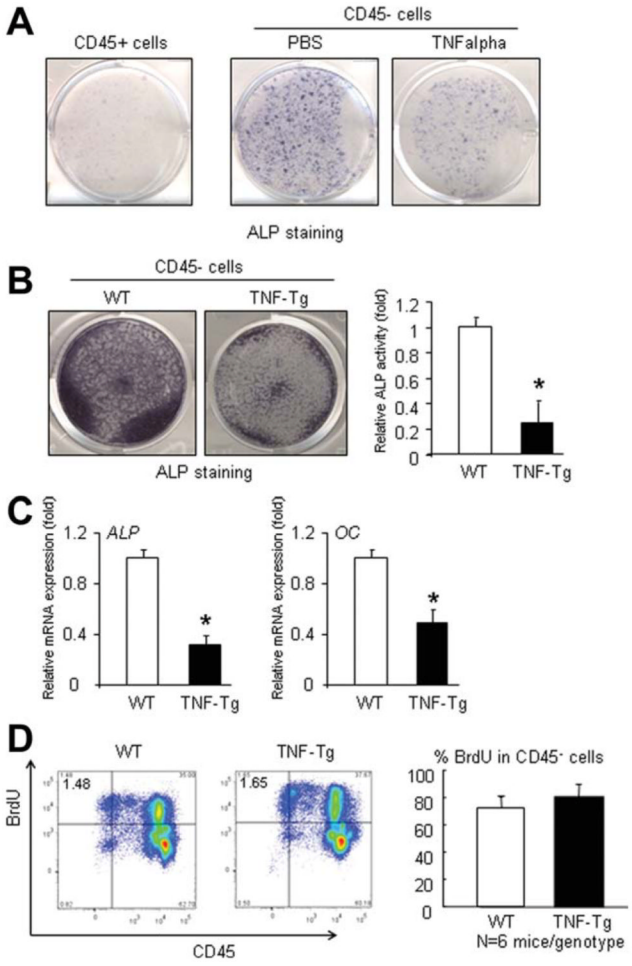

Figure 3.

Mesenchymal stem cell (MSC)-enriched CD45⁻ cells derived from TNF-Tg mice have decreased osteoblast differentiation. **(A):** MSC-enriched CD45⁻ cells isolated from BMSCs of wild-type (WT) mice were cultured in the osteoblast differentiation medium with or without TNF (7.5 ng/ml). Alkaline phosphatase (ALP) staining was performed after 4 days of culture. **(B):** CD45⁻ MSC-enriched cells isolated from BMSCs of TNF-Tg mice and WT littermates were cultured in the osteoblast differentiation medium plus 20 ng/ml BMP-2 for 10 days. Cells were subjected to ALP staining and ALP activity measurement and **(C)** osteoblast marker gene expressions of CD45⁻ cells were measured by real time-polymerase chain reaction. ALP activity was normalized to the total protein concentration for each sample. The relative ALP activity or gene expression levels was calculated by dividing the value from TNF-Tg cells by the values from WT cells which were normalized to 1. Values are the mean ± SD of four wells. *, $p < .05$ versus WT mice. The experiments were repeated three times with similar results. **(D):** TNF-Tg mice and WT littermates were injected with BrdU and harvested BMSCs were subjected to flow cytometry. The percentage of BrdU positive cells in the CD45⁻ cells was calculated. The values are the mean + SD of six mice per genotype. Abbreviations: ALP, alkaline phosphatise; OC, osteocalcin; PBS, phosphate buffered saline; TNF, tumor necrosis factor; WT, wild-type.

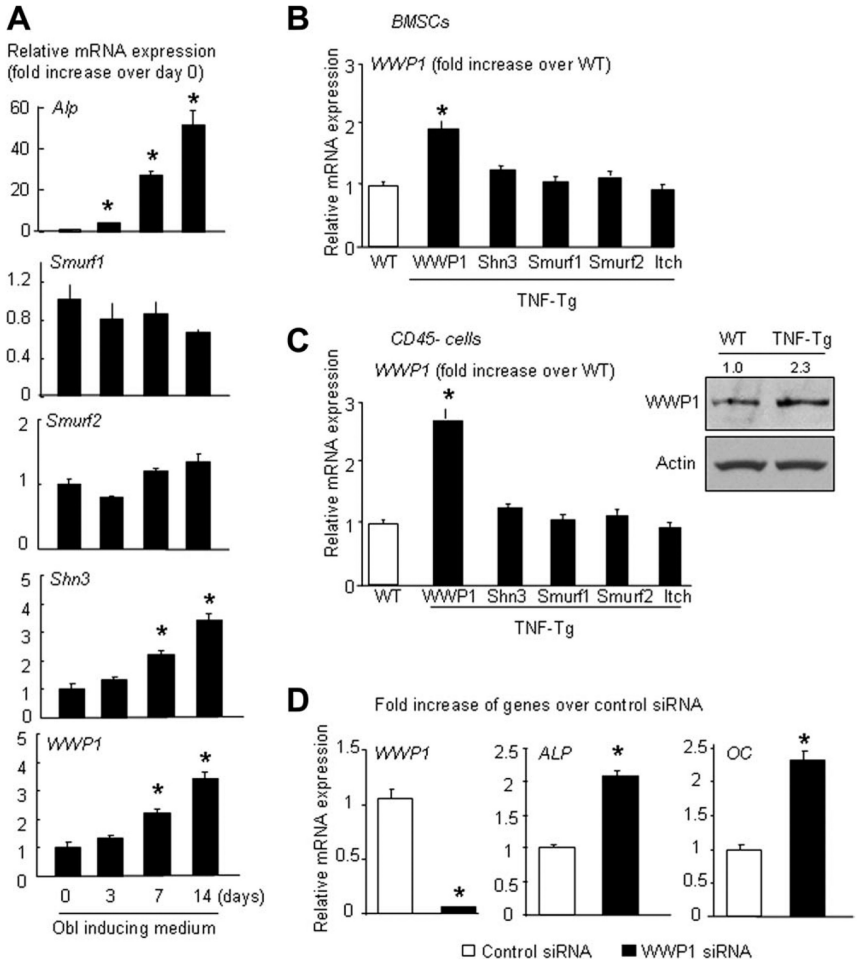

Figure 4.

Increased expression of the E3 ligase Wwp1 in bone marrow stromal cell (BMSCs) and MSC-enriched CD45$^-$ cells of TNF-Tg mice. **(A):** BMSCs harvested from wild-type (WT) mice were cultured in the osteoblast differentiation medium for the indicated time. The expression levels of E3 ligases were measured by real time-polymerase chain reaction (RT-PCR.) The fold increase was calculated by dividing the values of different groups by the value of day 0 which was normalized to 1. The values are the mean + SD of triplicates. **(B, C):** The expression levels of E3 ligases in BMSCs **(B)** and MSC-enriched CD45$^-$ cells **(C)** of TNF-Tg mice and WT littermates were determined by real time-polymerase chain reaction. The fold increase was calculated by dividing the value of the gene of interest by the value of the same gene from WT cells which was normalized to 1. The values are the mean + SD of triplicates. The Wwp1 protein level of CD45$^-$ cells was determined by Western blot analysis (inset). Fold change of Wwp1 protein was quantified using Image J and normalized to actin levels. **(D):** MSC-enriched CD45$^-$ cells from TNF-Tg mice were transfected with *Wwp1* siRNA or control siRNA, and 2 days after transfection, cells were cultured in the osteoblast differentiation medium with BMP-2 (200 ng/ml) for 4 days. The expression levels of the gene of interest were examined by RT-PCR. The values are the mean + SD of three wells. The fold increase was calculated by dividing the values of *Wwp1* siRNA-transfected cells by the value of control siRNA-transfected cells which was normalized to 1. *, $p < .05$ versus WT cells or control siRNA. The experiments were repeated three times with similar

results. Abbreviations: ALP, alkaline phosphatase; BMSC, bone marrow stromal cell; OC, osteocalcin; siRNA, small interfering RNA; TNF, tumor necrosis factor; WT, wild-type.

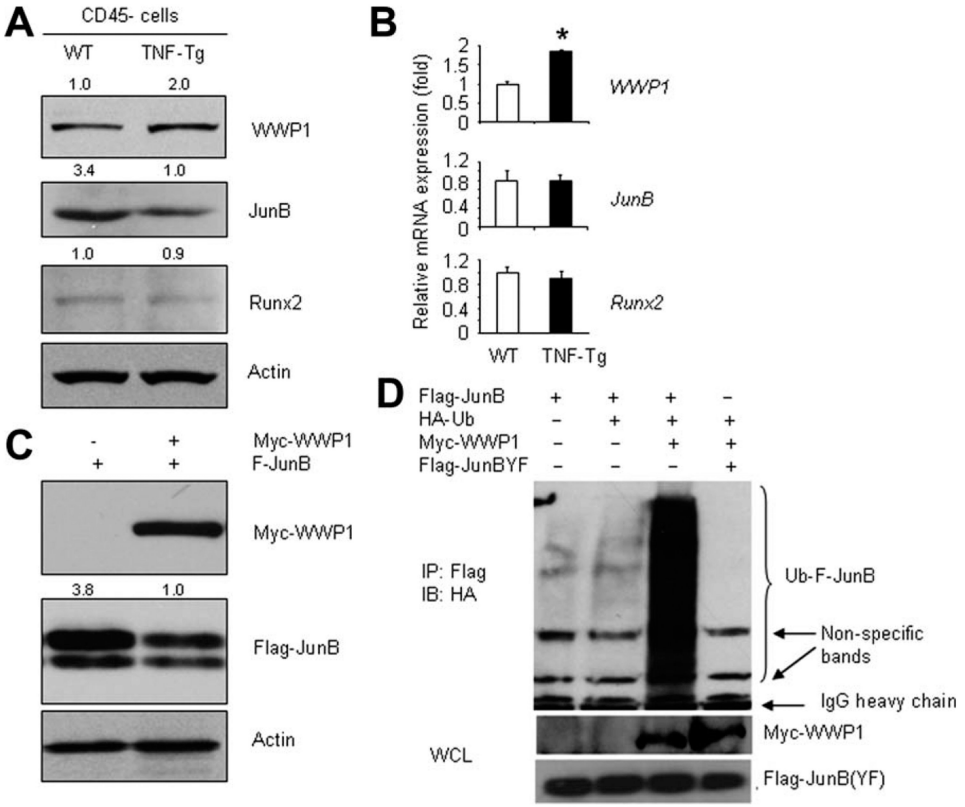

Figure 5.

Wwp1 induces JunB ubiquitination and degradation. **(A):** The expression levels of Wwp1, JunB, and Runx2 protein in mesenchymal stem cell (MSC)-enriched CD45$^-$ cells were examined by Western blot analysis. Fold changes were quantified using Image J and normalized to actin levels. **(B):** The expression levels of *Wwp1*, *JunB* and *Runx2* mRNA in MSC-enriched CD45$^-$ cells were examined by real time-polymerase chain reaction (RT-PCR). The fold increase was calculated by dividing the values of TNF-Tg cells by the value of wild-type cells which was defined as 1. The values are the mean + SD of three wells. **(C):** 293T cells were transfected with Myc-Wwp1 and Flag-JunB expression plasmids for 48 hours. The expression of transfected Wwp1 and JunB was determined by anti-Myc and anti-Flag antibodies, respectively. Fold change of Flag-JunB was quantified using Image J and normalized to actin level. **(D):** 293T cells were transfected with Myc-Wwp1, hemagglutinin (HA)-ubiquitin, Flag-JunB, or JunB-PY mutant for 48 hours and treated with MG132 (10 μM) in the last 4 hours. Cell lysates were subjected to IP with anti-Flag antibody and blotted with anti-HA to detect ubiquitinated JunB protein. The experiments were repeated three times with similar results. Abbreviations: TNF, tumor necrosis factor; WT, wild-type.

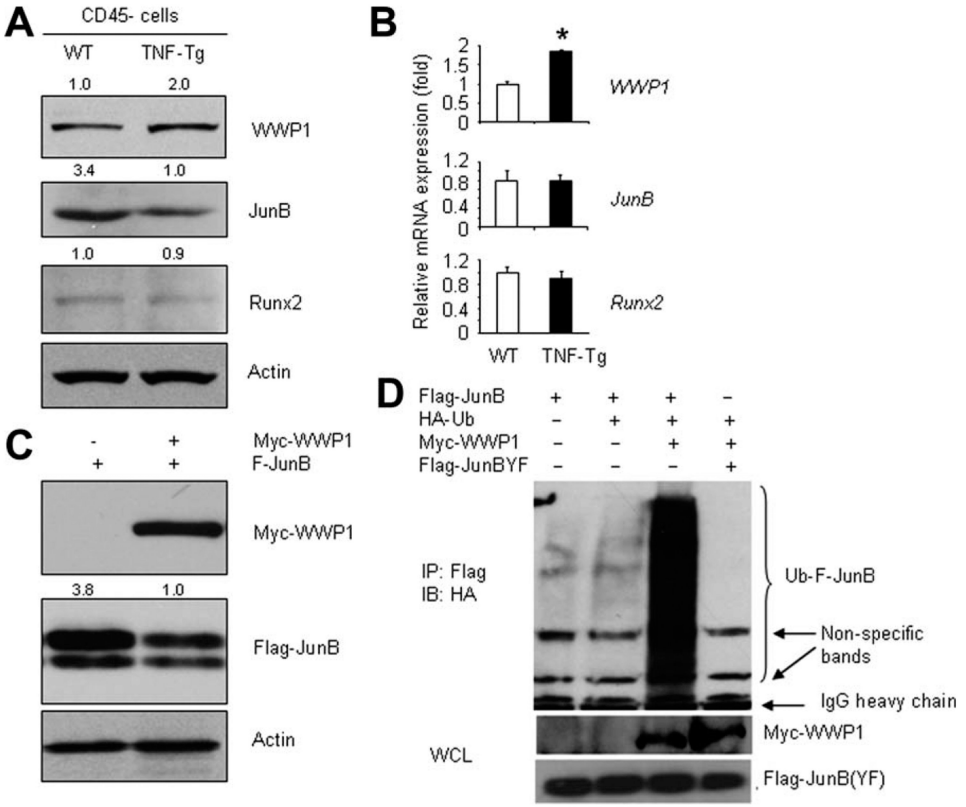

Figure 6.

TNF-induced mesenchymal stem cell (MSC) inhibition and JunB ubiquitination is abolished in Wwp1$^{-/-}$ mice. Wwp1$^{-/-}$ and wild-type (WT) mice were injected with either PBS or TNF as described in Figure 1. Bone marrow stromal cells (BMSCs) were subjected to colony-forming unit (CFU) assay, osteoblast marker gene expression, and JunB ubiquitination. **(A):** The numbers of CFU-F (eosin staining) colonies were counted and normalized to PBS-injected WT mice (which was set at 100%). Bars represent mean ± SD of four dishes per genotype. **(B):** *ALP* and *OC* mRNA levels of BMSCs from injected WT and *Wwp1*$^{-/-}$ mice were examined using quantitative RT-PCR. The values are mean ± SD of four dishes per genotype. **(C):** BMSCs derived from WT and *Wwp1*$^{-/-}$ mice injected with either PBS or TNF were treated with MG 132 (10 μM) for 4 hours and then lysed for ubiquitination assays to detect endogenous ubiquitinated JunB proteins. *, $p < .05$ versus PBS-injected WT. $n = 4$ per genotype. Abbreviations: ALP, alkaline phosphatase; CFU, colony-forming unit; OC, osteocalcin; PBS, phosphate buffered saline; TNF, tumor necrosis factor; WT, wild-type.

Table 1
Sequences of Primers Used in the Real-Time Polymerase Chain Reaction

Genes	Sequences of primers	GenBank accession number	Product sizes (bp)
Smurf1	F: 5′ AGTTCGTGGCCAAATAGTGG 3′	NM_001038627	99
	R: 5′ GTTCCTTCGTTCTCCAGCAG 3′		
Smurf2	F: 5′ TGTAACACAGGCAAATCCCA 3′	NM_025481	255
	R: 5′ CGACGTGGGGACAGATAAAT 3′		
Shn3	F: 5′ ACTCCCGTGTTTACCTCCC 3′	NM_010657	180
	R: 5′ GAACCCCTTCTTGGTCTTTT 3′		
Itch	F: 5′ TCACTTGGGCATAGGTCTCT 3′	NM_008395	129
	R: 5′ TGTGCCCAGACACTGAGTTA 3′		
Wwp1	F: 5′ AGAATGGAGACCCTGCAACAAG 3′	NM_177327	104
	R: ′ GCAGGAGTTGGGAACAACAGTA 3′		
JunB	F: 5′ ATGTGCACGAAAATGGAACA 3′	NM_008416	217
	R: 5′ CCTGACCCGAAAAGTAGCTG 3′		
Runx2	F: 5′ CAAGAAGGCTCTGGCGTTTA 3′	NM_009820	81
	R: 5′ TGCAGCCTTAAATGACTCGG 3′		
ALP	F: 5′ CGGGACTGGTACTCGGATAA 3′	AF_285233	157
	R: 5′ ATTCCACGTCGGTTCTGTTC ′		
OC	F: 5′ CTTGGTGCACACCTAGCAGA 3′	AH_004426	186
	R: 5′ CTCCCTCATGTGTTGTCCCT 3′		

Abbreviations: F, forward primer; R, reverse primer.